



## NRC Publications Archive Archives des publications du CNRC

### **Simultaneous determination of structures, vibrations, and frontier orbital energies from a self-consistent range-separated hybrid functional**

Tamblyn, Isaac; Refaely-abramson, Sivan; Neaton, Jeffrey B.; Kronik, Leeor

This publication could be one of several versions: author's original, accepted manuscript or the publisher's version. / La version de cette publication peut être l'une des suivantes : la version prépublication de l'auteur, la version acceptée du manuscrit ou la version de l'éditeur.

For the publisher's version, please access the DOI link below. / Pour consulter la version de l'éditeur, utilisez le lien DOI ci-dessous.

#### **Publisher's version / Version de l'éditeur:**

<https://doi.org/10.1021/jz5010939>

*The Journal of Physical Chemistry Letters*, 5, 15, pp. 2734-2741, 2014-08-07

#### **NRC Publications Record / Notice d'Archives des publications de CNRC:**

<https://nrc-publications.canada.ca/eng/view/object/?id=b4354087-b275-4f95-bd13-295106a04672>

<https://publications-cnrc.canada.ca/fra/voir/objet/?id=b4354087-b275-4f95-bd13-295106a04672>

Access and use of this website and the material on it are subject to the Terms and Conditions set forth at

<https://nrc-publications.canada.ca/eng/copyright>

READ THESE TERMS AND CONDITIONS CAREFULLY BEFORE USING THIS WEBSITE.

L'accès à ce site Web et l'utilisation de son contenu sont assujettis aux conditions présentées dans le site

<https://publications-cnrc.canada.ca/fra/droits>

LISEZ CES CONDITIONS ATTENTIVEMENT AVANT D'UTILISER CE SITE WEB.

**Questions?** Contact the NRC Publications Archive team at

PublicationsArchive-ArchivesPublications@nrc-cnrc.gc.ca. If you wish to email the authors directly, please see the first page of the publication for their contact information.

**Vous avez des questions?** Nous pouvons vous aider. Pour communiquer directement avec un auteur, consultez la première page de la revue dans laquelle son article a été publié afin de trouver ses coordonnées. Si vous n'arrivez pas à les repérer, communiquez avec nous à PublicationsArchive-ArchivesPublications@nrc-cnrc.gc.ca.



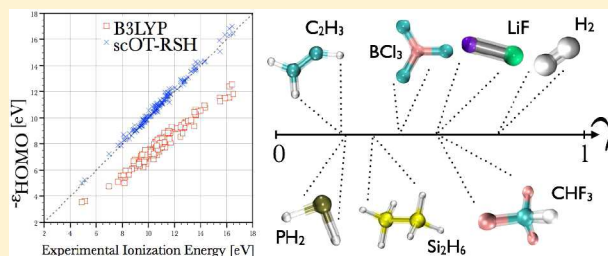
# Simultaneous Determination of Structures, Vibrations, and Frontier Orbital Energies from a Self-Consistent Range-Separated Hybrid Functional

Isaac Tamblyn,<sup>\*,†</sup> Sivan Refaely-Abramson,<sup>‡</sup> Jeffrey B. Neaton,<sup>¶,§,||</sup> and Leeor Kronik<sup>‡</sup><sup>†</sup>Department of Physics, University of Ontario Institute of Technology, Oshawa, Ontario L1H 7K4, Canada<sup>‡</sup>Department of Materials and Interfaces, Weizmann Institute of Science, Rehovoth 76100, Israel<sup>¶</sup>Molecular Foundry, Lawrence Berkeley National Laboratory, Berkeley, California 94720, United States<sup>§</sup>Department of Physics, University of California, Berkeley, California 94720, United States<sup>||</sup>Kavli Energy Nanosciences Institute at Berkeley, Berkeley, California 94720, United States

## S Supporting Information

**ABSTRACT:** A self-consistent optimally tuned range-separated hybrid density functional (scOT-RSH) approach is developed. It can simultaneously predict accurate geometries, vibrational modes, and frontier orbital energies. This is achieved by optimizing the range-separation parameter,  $\gamma$ , to both satisfy the ionization energy theorem and minimize interatomic forces. We benchmark our approach against an established hybrid functional, B3LYP, using the G2 test set. scOT-RSH greatly improves the accuracy of occupied frontier orbital energies, with a mean absolute error (MAE) of only 0.2 eV relative to experimental ionization energies compared to 2.96 eV with B3LYP. Geometries do not change significantly compared to those obtained from B3LYP, with a bond length MAE of 0.012 Å compared to 0.008 Å for B3LYP, and a 6.5% MAE for zero-point energies, slightly larger than that of B3LYP (3.1%). scOT-RSH represents a new paradigm in which accurate geometries and ionization energies can be predicted simultaneously from a single functional approach.

**SECTION:** Molecular Structure, Quantum Chemistry, and General Theory



Density functional theory (DFT) is the method of choice for electronic-structure calculations across an unusually wide variety of disciplines,<sup>1</sup> from organic chemistry<sup>2</sup> to condensed matter physics,<sup>3</sup> as it allows for accurate quantum-mechanical calculations at relatively modest computational cost. Practical applications of DFT almost invariably rely on the solution of the Kohn–Sham equation (in either its original<sup>4</sup> or generalized<sup>5</sup> form). Within (generalized) Kohn–Sham theory, the interacting many-electron problem is mapped onto an effective single-particle one. This mapping is exact in principle, as the ground-state density of the original and single-particle description are the same. However, the mapping relies on an exchange–correlation energy,  $E_{xc}$ , which is a generally unknown functional of the electron density. The practical success of DFT, therefore, hinges entirely on the existence of suitable approximations for  $E_{xc}$ .

Fortunately, approximations sufficiently accurate to predict quantities obtained from the total energy (including its first and second derivatives with respect to atomic positions) have been developed and are in widespread use. In particular, the generalized-gradient approximation (GGA), which expresses  $E_{xc}$  in terms of the electron density and its gradient, has become very popular in materials physics<sup>6</sup>—particularly when paired with periodic boundary conditions—and conventional hybrid

functionals, which combine a fraction of Fock exchange with a complementary fraction of GGA exchange, have seen similar rates of adoption for applications in chemistry.<sup>2</sup> These have become the standard “workhorse approximations” for accurate prediction of structural quantities such as lattice constants, bond lengths and angles, as well as response properties such as vibrational frequencies, elastic constants, etc.

Unfortunately, neither conventional GGAs nor conventional hybrid functionals do nearly as well in the prediction of electronic excitation spectra of molecular systems.<sup>7</sup> In particular, they usually fail to describe frontier orbital energies.<sup>8–11</sup> Within the (generalized) Kohn–Sham framework, the ionization energy (IE) theorem guarantees that for the exact exchange–correlation functional, the (generalized) Kohn–Sham eigenvalue associated with the highest occupied molecular orbital (HOMO) should correspond to the first vertical IE.<sup>9,12–16</sup> There are, however, no formal constraints on any of the other Kohn–Sham energies; for example, the lowest unoccupied molecular orbital (LUMO) energy computed from

Received: May 30, 2014

Accepted: July 15, 2014

Published: July 15, 2014

Kohn–Sham DFT is *not* guaranteed to correspond to the electron affinity (EA). In fact, the LUMO energy and EA differ by the derivative discontinuity, that is, by a finite “jump” in energy associated with an integer increase in the number of electrons in the system that the exact Kohn–Sham potential must possess. With standard GGA approaches, this derivative discontinuity is missing and is erroneously averaged away. Consequently, HOMO and LUMO energies under- and overestimate the IE and EA, respectively.<sup>17–19</sup> The use of a fraction of nonlocal Fock exchange in conventional hybrid functionals mitigates the derivative discontinuity problem, as some of it is “absorbed” into the nonlocal Fock operator. However, HOMO and LUMO energies typically still under- and overestimate the IE and EA, respectively, just like in a GGA, albeit less severely,<sup>9,20</sup> limiting the utility of the (generalized) Kohn–Sham spectrum for predicting and understanding spectroscopy measurements.

In recent years, a promising new class of hybrid functionals has emerged—that of range-separated hybrid (RSH) functionals,<sup>21,22</sup> which are based on partitioning the Coulomb interaction in space. Many such partitioning schemes exist.<sup>23–28</sup> Perhaps the simplest one distinguishes between short- and long-range contributions through use of the error function, namely, using the relation  $(1/r) = (1/r)\text{erfc}(\gamma r) + (1/r)\text{erf}(\gamma r)$ , where  $r$  is the interelectron coordinate and  $\gamma$  is an adjustable length-scale. The two interaction ranges are then treated differently: in the functional used here, the short-range term is handled in a GGA manner, allowing for a local balance between exchange and correlation contributions. Meanwhile, the long-range term is handled in a Fock-like manner, which guarantees the correct  $\sim -1/r$  asymptotic behavior for isolated molecules, crucial for processes involving electron removal (ionization).

It has been recently demonstrated<sup>9,29,30</sup> that the RSH approach can improve the DFT eigenvalue prediction if the range separation parameter,  $\gamma$ , is optimally tuned (OT) so as to obey the IE theorem, that is, it minimizes the function

$$j(N; \gamma) = \varepsilon_{\text{HOMO}}^{\gamma}(N) + [E_{\text{gs}}(N - 1; \gamma) - E_{\text{gs}}(N; \gamma)] \quad (1)$$

where  $\varepsilon_{\text{HOMO}}^{\gamma}(N)$  is the eigenvalue of the highest occupied generalized Kohn–Sham state for the  $N$ -electron system, and  $E_{\text{gs}}(N; \gamma)$  and  $E_{\text{gs}}(N - 1; \gamma)$  are the total energies of the original system and its cation, respectively, for a specific choice of  $\gamma$ . The function  $j$  then represents the remaining deviation from the IE theorem, where  $j = 0$  implies that the HOMO level is equal (and opposite in sign) to the IE, as expected from the exact functional. Simultaneous excellent agreement between the LUMO and EA can be obtained by applying the above condition not only on the neutral system but also on its anion,<sup>9,29</sup> for example, to minimize

$$J(N; \gamma) = \sqrt{[j(N; \gamma)]^2 + [j(N + 1; \gamma)]^2} \quad (2)$$

This double-tuning procedure has been used successfully for predicting fundamental (with time-independent DFT) and optical gaps (with time-dependent DFT) in a variety of systems (see, for example, refs 30–42). Additionally, it was shown to be useful in the prediction of other optical properties such as (full, partial, or implicit) charge-transfer excitations<sup>29,43–47</sup> and optical rotations.<sup>48</sup> It has also proven to be helpful beyond the frontier orbital energies in approximating the outer valence excitation spectra.<sup>49,50</sup> It should be noted, however, that the

double-tuning procedure should not be applied when the EA is negative.<sup>31</sup>

Despite this impressive range of successes, structural information in most of the above-mentioned OT-RSH research was obtained using conventional semilocal or hybrid functionals, with the relaxed geometry “frozen” for the sake of the subsequent OT-RSH calculation. Very little work has been devoted to structural predictions from OT-RSH calculations.<sup>33,51–53</sup> Apart from our preliminary results,<sup>54</sup> and the work of Körzdörfer et al.,<sup>55</sup> which focused on the specific case of bond-length alternation in polyenes, tuning of  $\gamma$  and structural optimization have been treated as unrelated tasks.

Generally speaking, obtaining a functional that offers predictions of sufficient accuracy for quantities derived from *both* the total energy and the frontier orbital eigenvalues is known to be a very difficult task.<sup>56–60</sup> Therefore, it is of great interest to examine whether, and to what extent, OT-RSH functionals can balance these two requirements. Specifically, we ask whether OT-RSH functionals can supply accurate predictions for both frontier orbital eigenvalues on the one hand and structures and vibrational frequencies on the other hand.

In this Letter, we develop a self-consistent (scOT-RSH) approach for a nonempirical range-separated hybrid density functional that can simultaneously predict accurate geometries, vibrational modes, and frontier orbital energies of molecules. Starting with a range-separated hybrid functional, we introduce a scheme by which the range separation parameter  $\gamma$  can be simultaneously optimized to both satisfy the IE theorem and minimize the forces acting on atoms for molecular structures.

In order to assess our approach, we focus on the G2 test set,<sup>61</sup> which contains 148 small organic molecules. We have chosen this particular test set for two reasons. First, experimental gas-phase structural, vibrational, and ionization energy data have been extensively recorded for this set, making a comprehensive comparison between theory and experiment meaningful. Second, we compare our calculations to those obtained from the popular conventional hybrid functional, B3LYP.<sup>62,63</sup> In its construction, B3LYP was explicitly fit against thermochemistry data of this set and is therefore at its best by definition. This makes the burden of proof on the accuracy of our approach particularly high.

Our nonempirical range-separated hybrid density functional scheme proceeds as follows. First, following the existing OT-RSH approach,<sup>9,29</sup> for fixed geometry, we obtain the range separation parameter  $\gamma$  such that the molecule, in its fixed configuration, satisfies eq 1. Ten independent calculations (in parallel) for both the neutral and cationic species were performed at the initial geometry over a range of  $\gamma$  values. From these, the two values of  $\gamma$  most closely satisfying eq 1 were identified and then used as the upper and lower bound for a second trial set of ten  $\gamma$  values. All molecules exhibited a clear minimum of  $j(N; \gamma)$ . We note, however, that some molecules within the set require careful identification of their (neutral or cationic) ground-state spin configurations<sup>50,64,65</sup> (which can be quite sensitive to initial geometries, as discussed below).

Second, we optimize the positions of the nuclei in the ground state, that is, we eliminate any residual Hellmann–Feynman forces. For the new geometry, we then recompute  $\gamma$ . This procedure continues until we converge on a  $\gamma$  for which all forces are negligible. This results in an optimized geometry obtained without resorting to empirical parameters. For most molecules in the set, self-consistency was achieved in a single

iteration. Throughout the entire set, self-consistency was always reached in less than four iterations. Our parallel implementation results in an additional factor of 2–3 in the time-to-solution compared to that of standard DFT functionals.

We used B3LYP/6-31G\*-optimized structures<sup>66,67</sup> as initial geometries for our scheme. To rule out any bias B3LYP may have imposed on our results, we randomly selected several molecules from the set, optimized their structure using the unified force field,<sup>68</sup> and confirmed that this did not impact the final results. All calculations were performed using the QChem 3.2 package.<sup>69</sup> The “G3Large”<sup>70</sup> basis set was used throughout. This basis set was chosen as it is defined for all atom types present in G2 and is also compatible with the G3/99 and G3/05 test sets. We additionally ascertained that results obtained with this basis set are consistent with those obtained using Dunning’s cc-pVTZ basis set.<sup>71</sup> The largest differences found between the two basis-sets were of the order of 1% for the HOMO levels, 0.1% for bond lengths, and 1% for vibrational frequencies. We used an OT-RSH functional of the form given in eq 1 based on the LC- $\omega$ PBE functional,<sup>25</sup> which employs a short-range version of the Perdew–Burke–Ernzerhof (PBE) GGA exchange functional<sup>72</sup> and PBE-GGA correlation.

We emphasize that any structural relaxation within DFT typically requires two nested self-consistent procedures: an outer one for the geometry and an inner one for the self-consistent solution of the electronic structure at a fixed geometry.<sup>73</sup> Here, an additional self-consistency cycle, nested in between the usual inner and outer ones, is the self-consistency in the choice of  $\gamma$ . This allows the functional to adapt itself to both the instantaneous geometry and electronic structure of the system. Thus, one may think of our approach as a special case of a nonempirical “fourth generation” density functional, where the functional is not and cannot be expressed explicitly, but rather is defined implicitly with the aid of a uniquely defined numerical procedure.<sup>64</sup>

Most molecules in the G2 set have a negative EA (our calculations indicate that this is the case for 116 out of the 148 molecules in the data set). For many of the molecules that have a positive EA, experimental data for the vertical EA are sparse and not always reliable. Therefore, we use the single HOMO-tuning condition of eq 1, rather than the double-tuning procedure of eq 2. Nevertheless, the consequences of double tuning are discussed further below.

A first and crucial test of the suggested approach is the comparison of HOMO eigenvalues to experimental IEs. In particular, the question is whether, as in the above-mentioned previous work, the method still facilitates the prediction of the IE or whether the simultaneous geometry optimization reduces the level of agreement between theory and experiment. Our comparison to experimental IEs is based primarily on the database of the National Institute of Standards and Technology.<sup>74</sup> However, some of the examined systems have multiple reported reference values, with a large deviation among these values. For other systems, the data set contains two different spin configurations, but only one reference value exists. In other cases yet, values reported in the database as vertical ionization energies are in fact adiabatic. For these cases, we used values collected directly from the literature. A detailed report is tabulated in the Supporting Information. Nevertheless, we caution that some errors in the experimental data may remain. With this in mind, a comparison of HOMO eigenvalues from our self-consistent RSH functional and from B3LYP,

against the experimental gas-phase ionization energies, is given graphically in Figure 1 and is summarized in Table 1.

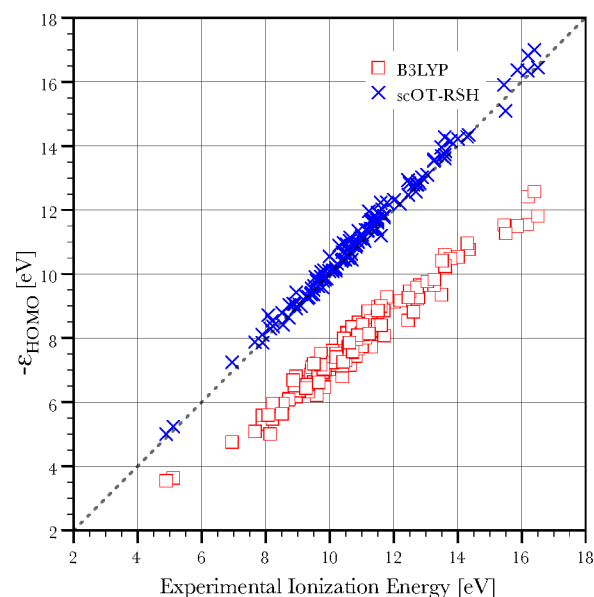


**Figure 1.** Comparison of the calculated generalized Kohn–Sham HOMO eigenvalues for the neutral species, calculated with B3LYP (red squares) and scOT-RSH (blue  $\times$  marks), with the experimental vertical ionization energy, in eV. Points lying on the 45° dashed line indicate agreement between theory and experiment (within the accuracy of the latter).

**Table 1. Comparison of Bond Lengths, HOMO Energies, and Zero-Point Energies Calculated Using B3LYP and the New scOT-RSH Scheme, with Experimental Values Across the G2 Set**

		HOMO [eV]	Bond length [Å]	ZPE [cm <sup>-1</sup> ]
scOT-RSH	MAE	0.20	0.012	379.31
	STD	0.17	0.014	299.4
	% error	1.84	1.02	6.49
B3LYP	MAE	2.96	0.008	250.73
	STD	0.52	0.011	258.4
	% error	27.24	0.61	3.10

Overall, and especially when considering the above-discussed difficulties in the comparison to experiment, the resulting mean absolute error (MAE) of the self-consistent functional HOMO energies with respect to experiment is excellent. The MAE is 0.2 eV, corresponding to a relative error of 1.84% from experiment, with a standard deviation (STD) of 0.17 eV. For comparison, B3LYP results severely underestimate the experimental values (as is well known and expected) and yield a MAE of 2.96 eV (i.e., a relative error of 27.24%) and a standard-deviation of 0.52 eV. Interestingly, recent work<sup>75</sup> explored the IEs of a subset of 55 molecules from the G2 set by applying various flavors of Koopmans’ corrections.<sup>16,76</sup> We note that our results are on par with the best results obtained from such corrections and slightly outperform the many-body perturbation theory results reported in ref 77 for a further subset of 34 of these 55 molecules.

It is important to note that IE predictions based on the B3LYP-optimized geometry, namely, a standard, nonself-consistent OT-RSH, differ from the scOT-RSH IE results by a very small amount (less than 0.01 eV). Importantly, although

the change in  $\gamma$  is modest in this case (less than 5%), all information can be extracted from one fully self-consistent DFT calculation without any empiricism. The fact that we observe only small differences between self-consistent and nonself-consistent calculations in this case may then serve as a validation of the assumption made in previous calculations, i.e., that it is acceptable to base the OT-RSH calculations on geometries optimized with standard functionals. One can certainly envision, however, that for more complex molecules quantitative and even qualitative differences may arise.

Next, we compare computed bond lengths and angles to experimental gas-phase structure, again taken from the NIST database.<sup>74</sup> The results are given graphically in Figure 2 and

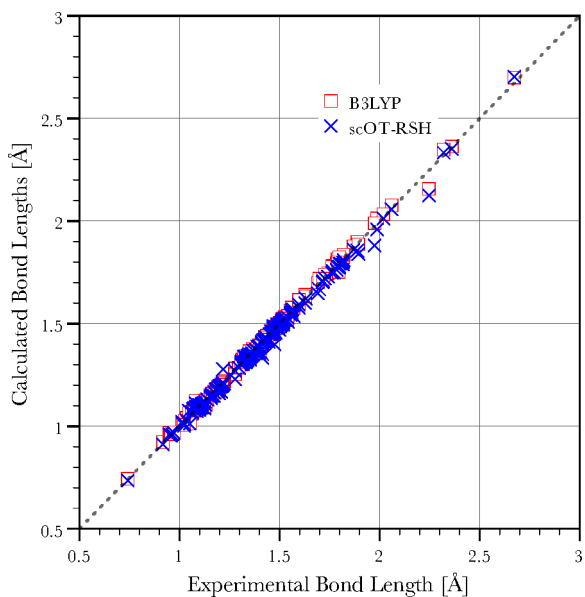


**Figure 2.** Comparison of theoretical bond lengths across the G2 test set, calculated with B3LYP (red squares) and scOT-RSH (blue × marks), with experimental values.<sup>74</sup> Points lying on the 45° dashed line indicate agreement between theory and experiment (within the accuracy of the latter).

summarized in Table 1. As expected, B3LYP bond-length predictions are within a highly satisfactory MAE of 0.008 Å from experiment (corresponding to a relative error of 0.61%), with a standard-deviation of 0.011 Å. The predicted bond lengths obtained from our self-consistent scheme exhibit a very similar accuracy, with a MAE of 0.012 Å from experiment (corresponding to a relative error of 1.02%) and a standard deviation of 0.014 Å. We additionally compared the self-consistent scheme predicted angles to experimental values. Again, in order to confine ourselves to well-established experimental data, we have limited our examination of angles to “central” ones within each molecule (see Supporting Information for further details). Here too, our results show a satisfying MAE of 0.52° from experiment, corresponding to a relative error of 0.48%. B3LYP results are very similar, with a MAE of 0.59° from experiment, corresponding to a relative error of 0.53%.

To further explore the capabilities of our suggested scheme, we examined molecular vibrational properties. For these calculations,  $\gamma$  was held fixed at the optimized value. This can be justified by assuming that  $\gamma$  is a weak function of the atomic positions (an assumption already verified above) so that its

change in the course of small-amplitude molecular vibrations can be neglected. Furthermore, allowing  $\gamma$  to change during the vibration raises difficulties associated with size-consistency issues, as discussed in detail below. To reduce the number of degrees of freedom and avoid spurious comparison of frequencies corresponding to different normal modes, we considered the zero-point energy (ZPE), calculated for each molecule by  $ZPE = 1/2 \hbar \sum_{\nu=0}^{M-1} \omega_{\nu}$ , where  $\hbar$  is the reduced Planck constant and  $\omega_{\nu}$  is the vibrational frequency for mode  $\nu$ , out of a total of  $M$  normal modes per molecule. The results, compared to ZPEs obtained from experimentally derived harmonic frequencies, are reported graphically in Figure 3 and

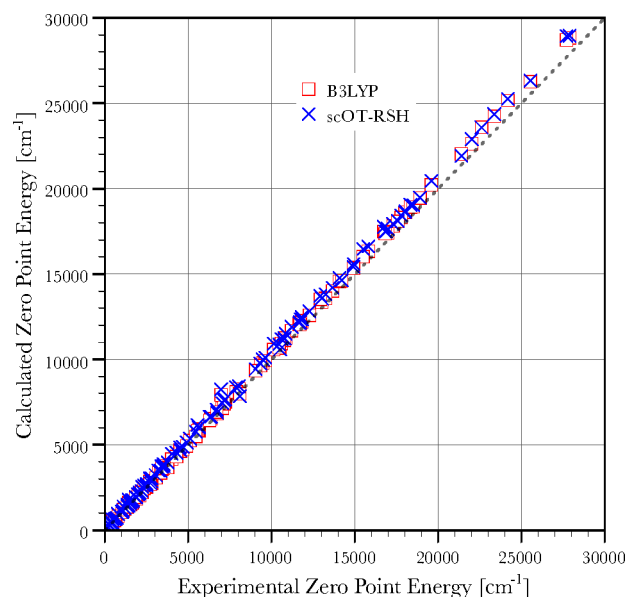


**Figure 3.** Comparison of theoretical zero-point energies across the G2 test set, calculated with B3LYP (red squares) and the new scOT-RSH scheme (blue × marks), with experimental values.<sup>74</sup> Points lying on the 45° dashed line indicate agreement between theory and experiment (within the accuracy of the latter).

summarized in Table 1. We find that B3LYP yield a MAE of 250.7 cm<sup>-1</sup>, corresponding to a relative error of 3.10% from experiment. Our self-consistent scheme yields a somewhat larger, but still useful, MAE of 379.3 cm<sup>-1</sup>, corresponding to a relative error of 6.49%.

The combined results of Figures 1–3 indicate that the suggested self-consistent scheme is indeed successful in predicting accurate HOMO energy levels across the G2 benchmark data set, without compromising the accuracy of structural predictions and with very little compromise on the accuracy of vibrational frequencies. Having established this overall success, we now turn to discussing present-day limitations of the approach.

First of all, trivially, the self-consistent approach hinges on success in finding an optimally tuned range-separation parameter,  $\gamma$ . This was possible for all molecules in the G2 data set. In some cases, issues with competing spin configurations arise, which manifest themselves in  $j(N;\gamma)$  with no minima. Special care must be taken in these instances to ensure that the spin configurations being used are indeed the optimized ones, namely, that they lead to the minimal total energy among all possible configurations.

Next, we address the issue of the detailed choice of tuning criterion. Specifically, we consider the difference between the single-tuning procedure of eq 1, recommended for determining ionization energies,<sup>26</sup> and the double-tuning procedure of eq 2, recommended for determining fundamental gaps as well as optical excitations.<sup>9,30</sup> As mentioned above, for most systems in the G2 data set the electron affinity is negative and eq 2 is inapplicable. However, for 32 molecules the self-optimized scheme based on eq 1 predicted a bound LUMO level. For these, we further investigated the effect of applying the double-tuning procedure. Recall that the minimal value of  $J$  in eq 2 may serve as a figure of merit for the expected remaining error in eigenvalues.<sup>78</sup> For 15 of the 32 examined molecules, the double-tuning procedure resulted in an optimal  $J$  smaller than 0.2 eV, that is, the prediction of both HOMO and LUMO energies is satisfactory. For 6 molecules, the double-tuning procedure led to a somewhat larger, but still tolerable, error of  $J = 0.2\text{--}0.3$  eV. For the remaining 11 molecules, the error was larger and in the range of  $J = 0.3\text{--}0.6$  eV, with one exception—OH—where the minimal  $J$  was 0.77 eV. Interestingly, among those 11 molecules, 10 are spin-polarized. In all these cases, we could easily find a value of  $\gamma$  such that the HOMO or LUMO tuning succeeds individually, that is, the first or second terms on the right-hand side of eq 2 are minimized separately. However, the value of  $\gamma$  needed for these two minimizations was too different to allow for a satisfactory least-squares compromise. Such behavior is typical for very small systems (and has been pointed out previously<sup>30,64</sup> for atoms and dimers), where the addition or removal of a single electron may change the chemical nature of the system strongly. This is typically much less of an issue for larger systems.<sup>9,30,50</sup> The good news is that the tuning procedure itself provides a warning sign when the reliability of the result may be suspect.

Generally speaking, the approximation we employ assumes an adequate choice for semilocal exchange and correlation expressions. If this is not the case, for example, due to significant contributions from static correlation<sup>55</sup> or long-range correlation,<sup>9,27,33,79</sup> results may suffer. This may be responsible for the slightly reduced accuracy in the description of molecular vibrations. Indeed, we found larger errors (of the order of 10%) for diatomic molecules, where left–right static correlation is important.<sup>80</sup> The combination of semilocal exchange and correlation is known to provide a mimic of static correlation effects.<sup>81,82</sup> In the RSH scheme, some of the semilocal exchange is replaced by Fock exchange by definition, which may explain some of the error. With B3LYP, however, molecules requiring more static correlation are part and parcel of the training set and the treatment is somewhat more accurate owing to the partial incorporation of such effects via the choice of semiempirical parameters.

Up to this point, we have discussed structural parameters and vibrational frequencies, which are related to the first and second derivative of the total energy, respectively. We have not, however, discussed atomization or reaction energies. These are related to finite total energy differences. In this case, the OT-RSH approach is at a disadvantage because of the size-consistency problem. The size consistency criterion is a fundamental constraint in DFT, which states that the total energy  $E_{AB}$  of a system comprised of two well-separated, independent subsystems A and B with energies  $E_A$  and  $E_B$  must be given by  $E_{AB} = E_A + E_B$ .<sup>6</sup> Nontuned RSH functionals are size consistent (as are all of their exchange and correlation ingredients). However, by construction, a tuned RSH func-

tional is not size consistent because, due to its implicit definition, it generally has different  $\gamma$  values for the whole system and the two separate subsystems. The size consistency error, defined as  $E_A + E_B - E_{AB}$ , where each of the energies is calculated with its own  $\gamma$ , tuned for the A, B, or AB system separately, was found to be as large as a few electronvolts for several diatomic molecules.<sup>64</sup> This drawback is particularly problematic for protonation/deprotonation processes, owing to the large  $\gamma$  associated with the hydrogen atom. Although in practice this is much less of an issue for larger fragments, theoretically this is a serious problem that is inherent in the methodology presented here.

Another possible difficulty with the new suggested scheme is the fact that while applying the self-consistent procedure, the resulting geometry may be affected by the specific value of  $\gamma$ , so that the self-consistent procedure can get “stuck” at a point that does not correspond to the stable ground-state configuration. If the total energy changes gradually with  $\gamma$ , which is usually found to be the case, this issue is not found to be a problem in practice. This can be learned from cases discussed above, where initial geometries from the unified force field led to exactly the same results as B3LYP initial geometries. However, this could be a severe issue for systems where different choices of  $\gamma$  lead to an abrupt change in the energy, typically owing to an abrupt change of electronic configuration.<sup>64</sup> For example, we found the optimal tuning of the P<sub>2</sub> molecule to be highly affected by the initial P–P bond length. Above some critical bond length, the tuning procedure did not succeed at all, likely due to a problematic configurations of the charged species within this larger separation. However, when starting with a smaller bond length the self-consistent procedure was normally applied and led to results that are well within the overall spread.

Even with these caveats, the results reported in Figures 1–3 represent, in our opinion, a major step forward. Our approach manages to obtain quantitatively useful information for quantities related to *both* eigenvalues and energies. The unique value of  $\gamma$ , obtained for each molecule, can be viewed as a descriptor for the character of the various electronic environments exhibited across the data set. Some selected molecules are shown and sorted by their optimal  $\gamma$  value in Figure 4. It has

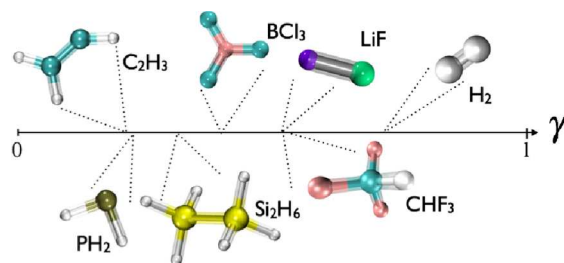


**Figure 4.** Selected molecules sorted by the optimal value of  $\gamma$  obtained through the scOT-RSH procedure.

been pointed out previously (e.g., in 30–32) that, within classes of chemically similar molecules,  $\gamma$  generally decreases with molecular size. This is a clear reflection of the fact that with increased electron delocalization the system emphasizes correlation over exchange. This immediately explains several additional features of our approach: First, the lack of a universal and arbitrary division between the relative importance of exchange and correlation, together with the fact that we wish to keep the expression for either one simple, is a strong driving

force for the use of a tuning procedure. Moreover, this immediately explains the repeated observation that results of a similar quality are not obtained with a fixed- $\gamma$  approach.<sup>9</sup> Second, the choice of  $\gamma$  from a physical consideration, rather than through fitting a data set, explains why we can approach the level of accuracy afforded by semiempirical functionals, even when the latter are given the “home field advantage”, that is, the comparison is made on the very data set used to parametrize the semiempirical approach. The obvious advantage is that, on general physical grounds, we expect the accuracy of our approach to remain similar for systems far removed from the benchmark data set, whereas this is not guaranteed for semiempirical approaches. In practice, one may still use initial geometries from other functionals in certain cases, but here we show that a fully self-consistent cycle is of the same level of accuracy. Finally, we note that in this self-consistent optimization approach, if long-range correlation is not essential, we can also expect other response properties to be well predicted.<sup>83</sup>

In conclusion, we have introduced and demonstrated the success of a self-consistent functional at describing geometrical and electronic properties across the 148 molecules in the G2 test set. Given that this approach contains no empirical or fitting parameters, its success at predicting experimental results establishes a new performance standard. Our implementation is fully parallelized and typically adds no more than a factor of 2 or 3 to the time-to-solution on a modern computing platform. Finally, the self-consistent procedure naturally produces an electronic order parameter that describes the varied nature of the electronic environment observed within the test set.

## ■ ASSOCIATED CONTENT

### ■ Supporting Information

Examples of internal angles considered, as well as alterations to ionization energies reported in the NIST database. This material is available free of charge via the Internet at <http://pubs.acs.org/>.

## ■ AUTHOR INFORMATION

### Corresponding Author

\*E-mail: [isaac.tamblyn@uoit.ca](mailto:isaac.tamblyn@uoit.ca)

### Notes

The authors declare no competing financial interest.

## ■ ACKNOWLEDGMENTS

We thank Roi Baer (Hebrew University, Jerusalem) for illuminating discussions. I.T. acknowledges support by NSERC and the Molecular Foundry. S.R.A. acknowledges support by an Adams fellowship of the Israel Academy of Sciences and Humanities. Work at the Weizmann Institute was supported by the European Research Council, the Israel Science Foundation, the United States–Israel Binational Science Foundation, the Helmsley Foundation, the Wolfson Foundation, and the Lise Meitner Minerva Center for Computational Chemistry. J.B.N. was supported by the U. S. Department of Energy, Office of Basic Energy Sciences, Division of Materials Sciences and Engineering (Theory FWP) under Contract No. DE-AC02-05CH11231. The work performed at the Molecular Foundry was also supported by the Office of Science, Office of Basic Energy Sciences, of the US Department of Energy. We thank the National Energy Research Scientific Computing Center for computational resources.

## ■ REFERENCES

- (1) Sholl, D. S.; Steckel, J. A. *Density Functional Theory: A Practical Introduction*; Wiley: Hoboken: NJ, 2009.
- (2) Koch, W.; Holthausen, M. C. *A Chemist's Guide to Density Functional Theory*; Wiley: Heidelberg: Germany, 2001.
- (3) Martin, R. M. *Electronic Structure: Basic Theory and Practical Methods*; Cambridge University Press: Cambridge UK, 2004.
- (4) Kohn, W.; Sham, L. J. Self-Consistent Equations Including Exchange and Correlation Effects. *Phys. Rev.* **1965**, *140*, A1133–A1138.
- (5) Seidl, A.; Görling, A.; Vogl, P.; Majewski, J. A.; Levy, M. Generalized Kohn–Sham Schemes and the Band-Gap Problem. *Phys. Rev. B* **1996**, *53*, 3764–3774.
- (6) Perdew, J. P.; Kurth, S. *A Primer in Density Functional Theory*; Springer-Verlag: Berlin, 2008; pp 1–51.
- (7) Kronik, L.; Kümmel, S. Gas-Phase Valence-Electron Photoemission Spectroscopy Using Density Functional Theory. *Topics in Current Chemistry* **2014**, DOI: 10.1007/128\_2013\_522.
- (8) Kümmel, S.; Kronik, L. Orbital-Dependent Density Functionals: Theory and Applications. *Rev. Mod. Phys.* **2008**, *80*, 3–60.
- (9) Kronik, L.; Stein, T.; Refaely-Abramson, S.; Baer, R. Excitation Gaps of Finite-Sized Systems from Optimally Tuned Range-Separated Hybrid Functionals. *J. Chem. Theory Comput.* **2012**, *8*, 1515–1531.
- (10) Onida, G.; Reining, L.; Rubio, A. Electronic Excitations: Density-Functional versus Many-Body Green'S-Function Approaches. *Rev. Mod. Phys.* **2002**, *74*, 601–659.
- (11) Louie, S. G.; Rubio, A. In *Handbook of Materials Modeling. Vol. I: Methods and Models*; Yip, S., Ed.; Springer: Berlin, 2005; pp 1–26.
- (12) Perdew, J. P.; Parr, R. G.; Levy, M.; Balduz, J. L. Density-Functional Theory for Fractional Particle Number: Derivative Discontinuities of the Energy. *Phys. Rev. Lett.* **1982**, *49*, 1691–1694.
- (13) Perdew, J. P.; Levy, M. Comment on “Significance of the Highest Occupied Kohn–Sham Eigenvalue”. *Phys. Rev. B* **1997**, *56*, 16021–16028.
- (14) Almladh, C.-O.; von Barth, U. Exact Results for the Charge and Spin Densities, Exchange-Correlation Potentials, And Density-Functional Eigenvalues. *Phys. Rev. B* **1985**, *31*, 3231–3244.
- (15) Levy, M.; Perdew, J. P.; Sahni, V. Exact Differential Equation for the Density and Ionization Energy of a Many-Particle System. *Phys. Rev. A* **1984**, *30*, 2745–2748.
- (16) Dabo, I.; Ferretti, A.; Poilvert, N.; Li, Y.; Marzari, N.; Cococcioni, M. Koopmans' condition for density-functional theory. *Phys. Rev. B* **2010**, *82*, 115121:1–16.
- (17) Perdew, J. P.; Levy, M. Physical Content of the Exact Kohn–Sham Orbital Energies: Band Gaps and Derivative Discontinuities. *Phys. Rev. Lett.* **1983**, *51*, 1884–1887.
- (18) Borgoo, A.; Teale, A. M.; Tozer, D. J. Effective Homogeneity of the Exchange–correlation and Non-Interacting Kinetic Energy Functionals under Density Scaling. *J. Chem. Phys.* **2012**, *136*, 034101–6.
- (19) But note recent work by Kraissler, E.; Kronik, L. *Phys. Rev. Lett.* **2013**, *110*, 126403; *J. Chem. Phys.* **2014**, *140*, 18A540. Armineto, R.; Kümmel, S. *Phys. Rev. Lett.* **2013**, *111*, 036402 on non-standard local-density approximation (LDA) and GGA application that allow for a derivative discontinuity to emerge even within these approximations.
- (20) Faber, C.; Boulanger, P.; Attacalite, C.; Duchemin, I.; Blase, X. Excited States Properties of Organic Molecules: From Density Functional Theory to the GW and Bethe–salpeter Green's Function Formalisms. *Philos. Trans. R. Soc. A* **2014**, *372*, 20130271–19.
- (21) Leininger, T.; Stoll, H.; Werner, H.-J.; Savin, A. Combining Long-Range Configuration Interaction with Short-Range Density Functionals. *Chem. Phys. Lett.* **1997**, *275*, 151–160.
- (22) Ikura, H.; Tsuneda, T.; Yanai, T.; Hirao, K. A Long-Range Correction Scheme for Generalized-Gradient-Approximation Exchange Functionals. *J. Chem. Phys.* **2001**, *115*, 3540–3544.
- (23) Yanai, T.; Tew, D. P.; Handy, N. C. A New Hybrid Exchange–Correlation Functional Using the Coulomb-Attenuating Method (CAM-B3LYP). *Chem. Phys. Lett.* **2004**, *393*, 51–57.

- (24) Baer, R.; Neuhauser, D. Density Functional Theory with Correct Long-Range Asymptotic Behavior. *Phys. Rev. Lett.* **2005**, *94*, 043002–4.
- (25) Vydrov, O. A.; Scuseria, G. E. Assessment of a Long-Range Corrected Hybrid Functional. *J. Chem. Phys.* **2006**, *125*, 234109–9.
- (26) Salzner, U.; Baer, R. Koopmans' Springs to Life. *J. Chem. Phys.* **2009**, *131*, 231101–4.
- (27) Refaely-Abramson, S.; Sharifzadeh, S.; Jain, M.; Baer, R.; Neaton, J. B.; Kronik, L. Gap Renormalization of Molecular Crystals from Density-Functional Theory. *Phys. Rev. B* **2013**, *88*, 081204–5.
- (28) Lucero, M. J.; Henderson, T. M.; Scuseria, G. E. Improved Semiconductor Lattice Parameters and Band Gaps from a Middle-Range Screened Hybrid Exchange Functional. *J. Phys.: Condens. Matter* **2012**, *24*, 145504–11.
- (29) Stein, T.; Kronik, L.; Baer, R. Reliable Prediction of Charge Transfer Excitations in Molecular Complexes Using Time-Dependent Density Functional Theory. *J. Am. Chem. Soc.* **2009**, *131*, 2818–2820.
- (30) Stein, T.; Eisenberg, H.; Kronik, L.; Baer, R. Fundamental Gaps in Finite Systems from Eigenvalues of a Generalized Kohn–Sham Method. *Phys. Rev. Lett.* **2010**, *105*, 266802–4.
- (31) Refaely-Abramson, S.; Baer, R.; Kronik, L. Fundamental and Excitation Gaps in Molecules of Relevance for Organic Photovoltaics from an Optimally Tuned Range-Separated Hybrid Functional. *Phys. Rev. B* **2011**, *84*, 075144–8.
- (32) Körzdörfer, T.; Sears, J. S.; Sutton, C.; Brédas, J.-L. Long-Range Corrected Hybrid Functionals for  $\pi$ -Conjugated Systems: Dependence of the Range-Separation Parameter on Conjugation Length. *J. Chem. Phys.* **2011**, *135*, 204107–6.
- (33) Salzner, U.; Aydin, A. Improved Prediction of Properties of  $\pi$ -Conjugated Oligomers with Range-Separated Hybrid Density Functionals. *J. Chem. Theory Comput.* **2011**, *7*, 2568–2583.
- (34) Phillips, H.; Zheng, S.; Hyla, A.; Laine, R.; Goodson, T.; Geva, E.; Dunietz, B. D. Ab Initio Calculation of the Electronic Absorption of Functionalized Octahedral Silsesquioxanes via Time-Dependent Density Functional Theory with Range-Separated Hybrid Functionals. *J. Phys. Chem. A* **2012**, *116*, 1137–1145.
- (35) Foster, M. E.; Wong, B. M. Nonempirically Tuned Range-Separated DFT Accurately Predicts Both Fundamental and Excitation Gaps in DNA and RNA Nucleobases. *J. Chem. Theory Comput.* **2012**, *8*, 2682–2687.
- (36) Koppen, J. V.; Hapka, M.; Szczęśniak, M. M.; Chalaśiński, G. Optical Absorption Spectra of Gold Clusters Au<sub>n</sub> ( $n = 4, 6, 8, 12, 20$ ) from Long-Range Corrected Functionals with Optimal Tuning. *J. Chem. Phys.* **2012**, *137*, 114302–15.
- (37) Risko, C.; Brédas, J. L. Small Optical Gap Molecules and Polymers: Using Theory to Design More Efficient Materials for Organic Photovoltaics. In *Topics in Current Chemistry*; Springer-Verlag: Berlin, 2013.
- (38) Jackson, N. E.; Savoie, B. M.; Kohlstedt, K. L.; Marks, T. J.; Chen, L. X.; Rathner, M. A. Structural and Conformational Dispersion in the Rational Design of Conjugated Polymers. *Macromolecules* **2014**, *47*, 987–992.
- (39) Phillips, H.; Zheng, Z.; Geva, E.; Dunietz, B. D. Orbital Gap Predictions for Rational Design of Organic Photovoltaic Materials. *Org. Electron.* **2014**, *15*, 1509–1520.
- (40) Sun, H.; Autschbach, J. Electronic Energy Gaps for  $\pi$ -Conjugated Oligomers and Polymers Calculated with Density Functional Theory. *J. Chem. Theory Comput.* **2014**, *10*, 1035–1047.
- (41) Foster, M. E.; Azoulay, J. D.; Wong, B. M.; Allendorf, M. D. Novel Metal–Organic Framework Linkers for Light Harvesting Applications. *Chem. Sci.* **2014**, *5*, 2081–2090.
- (42) Jacquemin, D.; Moore, B.; Planchat, A.; Adamo, C.; Autschbach, J. Performance of an Optimally Tuned Range-Separated Hybrid Functional for 0–0 Electronic Excitation Energies. *J. Chem. Theory Comput.* **2014**, *10*, 1677–1685.
- (43) Stein, T.; Kronik, L.; Baer, R. Prediction of Charge-Transfer Excitations in Coumarin-Based Dyes Using a Range-Separated Functional Tuned from First Principles. *J. Chem. Phys.* **2009**, *131*, 244119–5.
- (44) Sini, G.; Sears, J. S.; Brédas, J.-L. Evaluating the Performance of DFT Functionals in Assessing the Interaction Energy and Ground-State Charge Transfer of Donor/Acceptor Complexes: Tetrathiafulvalene-Tetracyanoquinodimethane (TTF-TCNQ) as a Model Case. *J. Chem. Theory Comput.* **2011**, *7*, 602–609.
- (45) Kuritz, N.; Stein, T.; Baer, R.; Kronik, L. Charge-Transfer-Like  $\pi \rightarrow \pi^*$  Excitations in Time-Dependent Density Functional Theory: A Conundrum and Its Solution. *J. Chem. Theory Comput.* **2011**, *7*, 2408–2415.
- (46) Karolewski, A.; Stein, T.; Baer, R. Tailoring the Optical Gap in Light-Harvesting Molecules. *J. Chem. Phys.* **2011**, *134*, 151101–4.
- (47) Phillips, H.; Geva, E.; Dunietz, B. D. Calculating Off-Site Excitations in Symmetric Donor–Acceptor Systems via Time-Dependent Density Functional Theory with Range-Separated Density Functionals. *J. Chem. Theory Comput.* **2012**, *8*, 2661–2668.
- (48) Srebro, M.; Autschbach, J. Tuned Range-Separated Time-Dependent Density Functional Theory Applied to Optical Rotation. *J. Chem. Theory Comput.* **2012**, *8*, 245–256.
- (49) Stein, T.; Autschbach, J.; Govind, N.; Kronik, L.; Baer, R. Curvature and Frontier Orbital Energies in Density Functional Theory. *J. Phys. Chem. Lett.* **2012**, *3*, 3740–3744.
- (50) Egger, D. A.; Weissman, S.; Refaely-Abramson, S.; Sharifzadeh, S.; Dauth, M.; Baer, R.; Kümmel, S.; Neaton, J. B.; Zojer, E.; Kronik, L. Outer-Valence Electron Spectra of Prototypical Aromatic Heterocycles from an Optimally Tuned Range-Separated Hybrid Functional. *J. Chem. Theory Comput.* **2014**, *10*, 1934–1952.
- (51) Moore, B.; Autschbach, J. Longest-wavelength electronic excitations of linear cyanines: The role of electron delocalization and of approximations in time-dependent density functional theory. *J. Chem. Theory Comput.* **2013**, *9*, 4991–5003.
- (52) Romanova, J.; Liégeois, V.; Champagne, B. Analysis of the Resonant Raman Spectra of Viologens and of Their Radical Cations Using Range-Separated Hybrid Density Functionals. *J. Phys. Chem. C* **2014**, *118*, 12469–12484.
- (53) Niskanen, M.; Hukka, T. I. Modeling of Photoactive Conjugated Donor–Acceptor Copolymers: the Effect of the Exact HF Exchange in DFT Functionals on Geometries and Gap Energies of Oligomer and Periodic Models. *Phys. Chem. Chem. Phys.* **2014**, *16*, 13294–13305.
- (54) Tamblyn, I.; Baer, R.; Kronik, L.; Neaton, J. B. *2011 March Meeting of the American Physical Society, Lecture Y24.0011*.
- (55) Körzdörfer, T.; Parrish, R. M.; Sears, J. S.; Sherrill, C. D.; Brédas, J.-L. On the Relationship between Bond-Length Alternation and Many-Electron Self-Interaction Error. *J. Chem. Phys.* **2012**, *137*, 124305–8.
- (56) Goedecker, S.; Umrigar, C. J. Critical Assessment of the Self-Interaction-Corrected–Local-Density-Functional Method and Its Algorithmic Implementation. *Phys. Rev. A* **1997**, *55*, 1765–1771.
- (57) Verma, P.; Bartlett, R. J. Increasing the Applicability of Density Functional Theory. II. Correlation Potentials from the Random Phase Approximation and Beyond. *J. Chem. Phys.* **2012**, *136*, 044105–8.
- (58) Schmidt, T.; Kraisler, E.; Kronik, L.; Kümmel, S. One-Electron Self-Interaction and the Asymptotics of the Kohn–Sham Potential: an Impaired Relation. *Phys. Chem. Chem. Phys.* **2014**, *16*, 14357–14367.
- (59) Schmidt, T.; Kraisler, E.; Makmal, A.; Kronik, L.; Kümmel, S. A Self-Interaction-Free Local Hybrid Functional: Accurate Binding Energies vis-à-vis Accurate Ionization Potentials from Kohn–Sham Eigenvalues. *J. Chem. Phys.* **2014**, *140*, 18A510–13.
- (60) Verma, P.; Bartlett, R. J. Increasing the Applicability of Density Functional Theory. IV. Consequences of Ionization-Potential Improved Exchange–Correlation Potentials. *J. Chem. Phys.* **2014**, *140*, 18A534–11.
- (61) Curtiss, L. A.; Redfern, P. C.; Raghavachari, K.; Pople, J. A. Assessment of Gaussian-2 and Density Functional Theories for the Computation of Ionization Potentials and Electron Affinities. *J. Chem. Phys.* **1998**, *109*, 42–55.
- (62) Becke, A. D. Density Functional Thermochemistry. III. The Role of Exact Exchange. *J. Chem. Phys.* **1993**, *98*, 5648–5652.
- (63) Stephens, P. J.; Devlin, F. J.; Chabalowski, C. F.; Frisch, M. J. Ab Initio Calculation of Vibrational Absorption and Circular Dichroism



Spectra Using Density Functional Force Fields. *J. Phys. Chem.* **1994**, *98*, 11623–11627.

(64) Karolewski, A.; Kronik, L.; Kümmel, S. Using Optimally Tuned Range Separated Hybrid Functionals in Ground-State Calculations: Consequences and Caveats. *J. Chem. Phys.* **2013**, *138*, 204115–11.

(65) For radicals, the problem of spin-contamination is well-known, and we can expect the same with our method. This was not examined here, as the results show that it did not degrade the quality of the predictions made significantly.

(66) Curtiss, L. A.; Raghavachari, K.; Redfern, P. C.; Pople, J. A. Assessment of Gaussian-2 and Density Functional Theories for the Computation of Enthalpies of Formation. *J. Chem. Phys.* **1997**, *106*, 1063–1079.

(67) Baboul, A. G.; Curtiss, L. A.; Redfern, P. C.; Raghavachari, K. Gaussian-3 Theory Using Density Functional Geometries and Zero-Point Energies. *J. Chem. Phys.* **1999**, *110*, 7650–7657.

(68) Rappe, A. K.; Casewit, C. J.; Colwell, K. S.; Goddard, W. A.; Skiff, W. M. UFF, a Full Periodic Table Force Field for Molecular Mechanics and Molecular Dynamics Simulations. *J. Am. Chem. Soc.* **1992**, *114*, 10024–10035.

(69) Shao, Y.; et al. Advances in Methods and Algorithms in a Modern Quantum Chemistry Program Package. *Phys. Chem. Chem. Phys.* **2006**, *8*, 3172–3191.

(70) Curtiss, L. A.; Raghavachari, K.; Redfern, P. C.; Rassolov, V.; Pople, J. A. Gaussian-3 (G3) Theory for Molecules Containing First and Second-Row Atoms. *J. Chem. Phys.* **1998**, *109*, 7764–7776.

(71) Dunning, T. H. Gaussian Basis Sets for Use in Correlated Molecular Calculations. I. The Atoms Boron through Neon and Hydrogen. *J. Chem. Phys.* **1989**, *90*, 1007–1023.

(72) Perdew, J. P.; Burke, K.; Ernzerhof, M. Generalized Gradient Approximation Made Simple. *Phys. Rev. Lett.* **1996**, *77*, 3865–3868.

(73) Payne, M. C.; Teter, M. P.; Allan, D. C.; Arias, T. A.; Joannopoulos, J. D. Iterative Minimization Techniques for Ab Initio Total-Energy Calculations: Molecular Dynamics and Conjugate Gradients. *Rev. Mod. Phys.* **1992**, *64*, 1045–1097.

(74) NIST Computational Chemistry Comparison and Benchmark Database, NIST Standard Reference Database Number 101 Release 16a; Johnson, III, R. D., Ed.; NIST: Gaithersburg, MD, 2013; <http://cccbdb.nist.gov/>.

(75) Borghi, G.; Ferretti, A.; Nguyen, N. L.; Dabo, I.; Marzari, N. Koopmans-Compliant Functionals and Their Performance against Reference Molecular Data. 2014, *arXiv:cond-mat/1405.4635*. [arXiv.org](http://arxiv.org/abs/1405.4635) e-Print archive. <http://arxiv.org/abs/1405.4635> (accessed June 2014) and *Phys. Rev. B*, in press.

(76) Ferretti, A.; Dabo, I.; Cococcioni, M.; Marzari, N. Bridging Density-Functional and Many-Body Perturbation Theory: Orbital-Density Dependence in Electronic-Structure Functionals. *Phys. Rev. B* **2014**, *89*, 195134–8.

(77) Rostgaard, C.; Jacobsen, K. W.; Thygesen, K. S. Fully Self-Consistent GW Calculations for Molecules. *Phys. Rev. B* **2010**, *81*, 085103–12.

(78) Stein, T.; Autschbach, J.; Govind, N.; Kronik, L.; Baer, R. Curvature and Frontier Orbital Energies in Density Functional Theory. *J. Phys. Chem. Lett.* **2012**, *3*, 3740–3744.

(79) Nénon, S.; Champagne, B.; Spassova, M. I. Assessing Long-Range Corrected Functionals with Physically-Adjusted Range-Separated Parameters for Calculating the Polarizability and the Second Hyperpolarizability of Polydiacetylene and Polybutatriene Chains. *Phys. Chem. Chem. Phys.* **2014**, *16*, 7083–7088.

(80) Handy, N. C.; Cohen, A. J. Left–Right Correlation Energy. *Mol. Phys.* **2001**, *99*, 403–412.

(81) Mok, D. K. W.; Neumann, R.; Handy, N. C. Dynamical and Nondynamical Correlation. *J. Phys. Chem.* **1996**, *100*, 6225–6230.

(82) Gritsenko, O. V.; Schipper, P. R. T.; Baerends, E. J. Exchange and Correlation Energy in Density Functional Theory: Comparison of Accurate Density Functional Theory Quantities with Traditional Hartree–Fock Based Ones and Generalized Gradient Approximations for the Molecules Li<sub>2</sub>, N<sub>2</sub>, F<sub>2</sub>. *J. Chem. Phys.* **1997**, *107*, 5007–5015.

(83) Srebro, M.; Autschbach, J. Does a Molecule-Specific Density Functional Give an Accurate Electron Density? The Challenging Case of the CuCl Electric Field Gradient. *J. Phys. Chem. Lett.* **2012**, *3*, 576–581.